Inorg. Chem. **2008**, *47*, 2356−2361

$La_6Br_{10}Fe$: A La_6Fe Octahedron with a Mixed M_6X_{12}/M_6X_8 Type Environment[⊥]

Chong Zheng,[*,‡] Hansjürgen Mattausch,[§] Constantin Hoch,[§] and Arndt Simon[§]

Department of Chemistry and Biochemistry, Northern Illinois University, DeKalb, Illinois 60115, and Max-Planck-Institut für Festkörperforschung, Heisenbergstrasse 1, D-70569 Stuttgart, Germany

Received June 22, 2007

The title compound was synthesized from La, $LaBr_3$, and Fe under Ar atmosphere at 800 °C. It crystallizes in space group $P4_1$ (No. 76) with lattice constants $a = 8.255(1)$ Å and $c = 30.033(6)$ Å. The structure features an isolated Fe-centered La_6 octahedron with all corners, 9 of its 12 edges, and 3 of its 8 triangular faces coordinated, bridged, or capped by Br atoms. The La_6Fe octahedron is significantly distorted, and the La coordination by Br atoms deviates from the common close-packing arrangements found in other reduced rare earth metal halides. Band structure, bonding, and physical properties of the compound have been investigated.

Introduction

Metal atom cluster chemistry has made tremendous progress in the past four decades. For the octahedral clusters, there are mainly two structure types, M_6X_{12} and M_6X_8, where M stands for a metal atom and X a ligand, usually a chalcogen or halogen atom.[1] In the M_6X_{12} cluster, all edges of the M_6 octahedron are bridged by the X atoms. In the M_6X_8 cluster, all faces are capped by X atoms. These clusters can be linked or condensed to chains, sheets or three-dimensional frameworks.[2–8] In reduced rare earth (RE) metal halide compounds, a third interstitial atom can occupy the center of the cluster, making their electronic structures even more interesting. The structures of many reduced rare earth metal halides thus feature RE_6 octahedra centered by a great number of main group or transition metal atoms.[9–22] Among this remarkably large family of compounds, several members with Fe as interstitial have been reported. These include $Pr_7I_{12}Fe$, $Gd_7I_{12}Fe$, $Y_7I_{12}Fe$, $La_{12}I_{17}Fe_2$, $Pr_{12}I_{17}Fe_2$, and Gd_2Fe_2I.[17,23–26] The first five contain isolated RE_6Fe octahedral clusters. The latter features a condensed trigonal prism structure. In this contribution, we present a structure, bonding,

[⊥] Dedicated to Prof. Roald Hoffmann on the occasion of his 70th birthday.

* Corresponding author. E-mail: zheng@cz.chem.niu.edu.
‡ Northern Illinois University.
§ Max-Planck-Institut für Festkörperforschung.

(1) Schäfer, H.; Schnering, H. G. *Angew. Chem.* **1964**, *76*, 833.
(2) Simon, A. *Angew. Chem., Int. Ed. Engl.* **1981**, *20*, 1. *Angew. Chem.* **1981**, *93*, 23.
(3) Chevrel, R.; Gougeon, P.; Potel, M.; Sergent, M. *J. Solid State Chem.* **1985**, *57*, 25.
(4) Hughbanks, T.; Hoffmann, R. *J. Am. Chem. Soc.* **1983**, *105*, 3528.
(5) Hughbanks, T.; Hoffmann, R. *J. Am. Chem. Soc.* **1983**, *105*, 1150.
(6) Simon, A. *Angew. Chem., Int. Ed. Engl.* **1988**, *27*, 159. *Angew. Chem.* **1988**, *100*, 163.
(7) Köhler, J.; Svensson, G.; Simon, A. *Angew. Chem., Int. Ed. Engl.* **1992**, *31*, 1437. *Angew. Chem.* **1992**, *104*, 1463.
(8) Vajenine, G. V.; Simon, A. *Inorg. Chem.* **1999**, *38*, 3463.
(9) Simon, A.; Mattausch, Hj.; Miller, G. J.; Bauhofer, W.; Kremer, R. K. Metal-Rich Halides. In *Handbook on the Physics and Chemistry of Rare Earths*; Elsevier Science Publishers: Amsterdam−London−New York−Tokyo, 1991; Vol. 15, pp 191.
(10) Mattausch, Hj.; Simon, A. *Angew. Chem., Int. Ed.* **1998**, *37*, 499. *Angew. Chem.* **1998**, *110*, 498.
(11) Mattausch, Hj.; Oeckler, O.; Simon, A. *Inorg. Chim. Acta* **1999**, *289*, 174.
(12) Warkentin, E.; Simon, A. *Rev. Chim. Miner.* **1983**, *20*, 488.
(13) Nagaki, D.; Simon, A.; Borrmann, H. *J. Less-Common Metals* **1989**, *156*, 193.
(14) Dorhout, P. K.; Payne, M. W.; Corbett, J. D. *Inorg. Chem.* **1991**, *30*, 4960.
(15) Llusar, R.; Corbett, J. D. *Inorg. Chem.* **1994**, *33*, 849.
(16) Hughbanks, T.; Rosenthal, G.; Corbett, J. D. *J. Am. Chem. Soc.* **1986**, *108*, 8289.
(17) Hughbanks, T.; Corbett, J. D. *Inorg. Chem.* **1988**, *27*, 2022.
(18) Hughbanks, T.; Corbett, J. D. *Inorg. Chem.* **1989**, *28*, 631.
(19) Meyer, G.; Wickleder, M. S. Simple and Complex Halides. In *Handbook on the Physics and Chemistry of Rare Earths*; Elsevier Science Publishers: Amsterdam−London−New York−Tokyo, 2000; Vol. 28, Chapter 177, pp 53.
(20) Corbett, J. D. *J. Chem. Soc., Dalton Trans.* **1996**, 575.
(21) Meyer, G. *Z. Anorg. Allg. Chem.* **2007**, *633*, 2537.
(22) Simon, A.; Mattausch, Hj.; Ryazanov, M.; Kremer, R. K. *Z. Anorg. Allg. Chem.* **2006**, *632*, 919.
(23) Sweet, L. E.; Roy, L. E.; Meng, F.; Hughbanks, T. *J. Am. Chem. Soc.* **2006**, *128*, 10193.
(24) Ruck, M.; Simon, A. *Z. Anorg. Allg. Chem.* **1993**, *619*, 327.
(25) Lulei, M.; Martin, J. D.; Corbett, J. D. *J. Solid State Chem.* **1996**, *125*, 249.
(26) Park, Y.; Corbett, J. D. *Inorg. Chem.* **1994**, *33*, 1705.

10.1021/ic701229q CCC: $40.75
Published on Web 03/05/2008

and physical property study of still another phase, $La_6Br_{10}Fe$, which is also characterized by discrete La_6Fe octahedral clusters. The cluster is neither a M_6X_{12} nor a M_6X_8 type. Its structure represents a new type which differs from other known compounds with the same stoichiometry $RE_6X_{10}Z$, $Pr_6Br_{10}Z$ (Z = Co, Ru, Os), $Y_6I_{10}Ru$, and $La_6I_{10}(C_2)$, in the coordination environment of cluster and its stacking.[15,18,27]

Experimental Section

Synthesis. La metal (sublimed, 99.99%; Alfa-Aesar, small pieces), $LaBr_3$, and Fe (99.99%; Aldrich) were used as starting materials. $LaBr_3$ was prepared by the reaction of La_2O_3 with concentrated HBr and NH_4Br, the product being dried under dynamic vacuum and purified twice by sublimation in a Ta container before use. Due to air and moisture sensitivity of the reactants and product, all handling was carried out under Ar atmosphere either in a glovebox or through the standard Schlenk technique.

The stoichiometric mixture (ca. 1.0 g) of the starting materials was arc-sealed in a Ta tube under Ar atmosphere. The Ta tube was then sealed inside a silica glass ampule under a vacuum of ca. 10^{-2} mbar. The reaction was carried out at 800 °C for 21 days. After the reaction, the ampule was quenched in water and then opened under Ar atmosphere. Many black polyhedral single crystals were observed in the product. The yield, estimated from a Guinier powder X-ray measurement, was nearly 100%. EDX analyses of these single crystals, using a JEOL JSM-6510LV scanning electron microscope, confirmed the presence of the component elements in the average atomic ratio of 6:10:1 (La:Br:Fe). The crystals oxidize in air within minutes to a white powder.

Structure Determination. The reaction product was ground to fine powder under Ar atmosphere and sealed in a glass capillary for phase identification by a modified Guinier technique[28] (Cu $K\alpha_1$: $\lambda = 1.54056$ Å; internal standard Si with $a = 5.43035$ Å; Fujifilm BAS-5000 image plate system). Single crystals were transferred to glass capillaries under Na-dried paraffin oil and sealed under Ar atmosphere. They were first examined by the precession technique before being characterized on a STOE IPDS diffractometer with monochromatized Ag K_α radiation ($\lambda = 0.56086$ Å). Absorption corrections were applied through the program XRED, XSHAPE.[29] The structure was solved with direct methods using the SIR97 program.[30] Full matrix least-squares refinement on F^2 was carried out using the SHELXTL package.[31]

The product compound crystallizes in the tetragonal space group $P4_1$ (No. 76) with lattice constants $a = 8.255(1)$ Å and $c = 30.033(6)$ Å. The structure has been checked for possible existence of higher symmetry by the program ADDSYM in the PLATON package.[32] No additional symmetry element was found. The mean $|E^2 - 1|$ is low at 0.567, and the $\overline{F_o^2} < \overline{F_c^2}$ value of 11.5 is very high for the weak reflections with $0 < F_c/F_c(\max) < 0.04$. Examination of the reciprocal space revealed that the crystal possesses a twinning by merohedry. By applying the twinning matrix of (0 1 0; 1 0 0; 0 0 −1) the R_1-factor converged to 0.0339.

Table 1. Crystal Data and Structure Refinement for $La_6Br_{10}Fe$[a]

formula weight	1688.41
temperature	293(2) K
wavelength	0.56086 Å
crystal system	tetragonal
space group	$P4_1$ (No. 76)
unit cell dimensions	$a = 8.255(1)$ Å $c = 30.033(6)$ Å
volume	2046.4(6) Å^3
Z	4
density (calculated)	5.480 Mg/m^3
absorption coefficient	17.248 mm^{-1}
θ range for data collection	1.95−24.20°
index ranges	$-12 \le h \le 12$, $-12 \le k \le 12$, $-43 \le l \le 43$
reflections collected	27112
independent reflections	6585 [R(int) = 0.0576]
completeness to $\theta = 24.20°$	99.1%
absorption correction	numerical[29]
max. and min. transmission	0.91064 and 0.50453
refinement method	Full-matrix least-squares on F^2
data/restraints/parameters	6585/1/156
goodness-of-fit on F^2	1.100
R indices (all data)[b]	$R1 = 0.0339$, $wR2 = 0.0860$
largest diff. peak and hole	1.758 and −1.474 e Å^{-3}

[a] The refinement is for a twin model with the twin matrix of (0 1 0; 1 0 0; 0 0 −1). [b] $R1 = \Sigma||F_o| - |F_c||/\Sigma F_o|$; $wR2 = [\Sigma[w(F_o^2 - F_c^2)^2]/\Sigma[w(F_o^2)^2]]^{1/2}$.

Table 2. Atomic Coordinates ($\times 10^4$) and Equivalent Isotropic Displacement Parameters (Å$^2 \times 10^3$) for $La_6Br_{10}Fe$[a]

Atom[b]	x	y	z	U(eq)
La(1)	2931(1)	1853(1)	3079(1)	14(1)
La(2)	7116(1)	2372(1)	3791(1)	15(1)
La(3)	8013(1)	3938(1)	1983(1)	13(1)
La(4)	2644(1)	2089(1)	6117(1)	14(1)
La(5)	6288(1)	−1541(1)	3197(1)	13(1)
La(6)	1150(1)	6961(1)	1872(1)	14(1)
Br(1)	4782(2)	5023(2)	3298(1)	19(1)
Br(2)	6445(2)	1738(2)	2722(1)	23(1)
Br(3)	1532(2)	3170(2)	5159(1)	19(1)
Br(4)	1222(2)	3592(2)	3846(1)	18(1)
Br(5)	8827(2)	611(2)	4553(1)	28(1)
Br(6)	3518(2)	8387(2)	6358(1)	19(1)
Br(7)	5436(2)	4080(2)	4534(1)	25(1)
Br(8)	2536(2)	2319(2)	7148(1)	22(1)
Br(9)	281(2)	4953(2)	2750(1)	26(1)
Br(10)	9715(2)	23(2)	3297(1)	21(1)
Fe	75(2)	4603(2)	6282(1)	11(1)

[a] U(eq) is defined as one-third of the trace of the orthogonalized U_{ij} tensor. [b] Wyckoff positions for all atoms are 4*a*.

Without applying the twinning law, the R_1 value could only be refined to 0.192. The two twin components have nearly 1:1 ratio. The crystallographic information including the fractional coordinates and selected bond lengths of the compound is listed in Tables 1−3.

Computational Study. The density of states (DOS) and band structure were computed using both the tight-binding extended Hückel method (EH)[33,34] and the self-consistent linear muffin-tin orbital local density approximation method (LDA) as implemented in the Stuttgart-TB-LMTO-ASA program.[35] Here, 64 k-points in the irreducible wedge of the Brillouin zone were used in the EH computations, and approximately, 50 k-points were used during the self-consistent convergence part in the LDA calculations. Scalar relativistic equation using the Barth−Hedin local exchange potential was used. Default basis set and Wigner−Seitz radii were used, and empty spheres added in the interstitials according to the standard

(27) Mattausch, Hj.; Hoch, C.; Simon, A. *Z. Anorg. Allg. Chem.* **2005**, *631*, 1423.
(28) Simon, A. *J. Appl. Crystallogr.* **1970**, *3*, 11.
(29) *XRED32 1.26, X-SHAPE 2.05*, Crystal Optimisation for Numerical Absorption Correction; Stoe & Cie. GmbH: Darmstadt, 2004.
(30) Altomare, A.; Burla, M. C.; Camalli, M.; Cascarano, G. L.; Giacovazzo, C.; Guagliardi, A.; Moliterni, A. G. G.; Polidori, G.; Spagna, R. *J. Appl. Crystallogr.* **1999**, *32*, 115.
(31) Sheldrick, G. M. *SHELXTL*, version 6.10; Bruker Analytical Instruments Inc.: Madison, Wisconsin, 2000.
(32) Spek, A. L. *Acta Crystallogr., Sec. A: Found. Crystallogr.* **1990**, *46*, C34.
(33) Hoffmann, R. *J. Chem. Phys.* **1963**, *39*, 1397.
(34) Whangbo, M. H.; Hoffmann, R.; Woodward, R. B. *Proc. R. Soc. London* **1979**, *A366*, 23.
(35) Andersen, O. K.; Jepsen, O. *Phys. Rev. Lett.* **1984**, *53*, 2571.

Table 3. Selected Interatomic Distances [Å] and Types in $La_6Br_{10}Fe$

atom contacts	distances	type[a]
Br(1)−La(1), −La(2), −La(4), −La(5)	3.101(2), 3.270(2), 3.094(2), 3.112(2)	e, i-i
Br(2)−La(1), −La(2), −La(5); −La(3)	3.094(2), 3.302(2), 3.063(2); 3.146(2)	f, i-a; a-i
Br(3)−La(1), −La(4), −La(5); −La(6)	3.072(2), 3.148(2), 3.040(2); 3.148(2)	f, i-a; a-i
Br(4)−La(1), −La(6); −La(2), −La(4)	3.059(2), 2.968(2); 3.539(2), 3.263(2)	e, i-a; a-i
Br(5)−La(2), −La(3); −La(1), −La(6)	3.057(2), 3.139(2); 3.670(3), 3.547(2)	e, i-a; a-i
Br(6)−La(3), −La(5); −La(2), −La(4)	2.966(2), 3.100(2); 3.557(2), 3.223(2)	e, i-a; a-i
Br(7)−La(2), −La(6); −La(3)	2.980(2), 3.163(2); 3.291(2)	e, i-a; a-i
Br(8)−La(3), −La(4), −La(6); −La(5)	3.162(2), 3.105(2), 3.209(2); 3.358(2)	f, i-a; a-i
Br(9)−La(3), −La(6); −La(1), −La(4)	3.085(2), 3.197(2); 3.509(2), 3.596(2)	e, i-a; a-i
Br(10)−La(1), −La(4), −La(2), −La(5)	3.123(2), 3.099(2), 3.251(2), 3.124(2)	e, i-i
La(1)−Fe	2.982(2)	
La(2)−Fe	2.896(2)	
La(3)−Fe	2.894(3)	
La(4)−Fe	3.007(2)	
La(5)−Fe	2.547(3)	
La(6)−Fe	2.414(3)	
La(1)−La(2)	4.086(1)	
La(1)−La(4)	4.107(1)	
La(1)−La(5)	3.956(1)	
La(1)−La(6)	3.927(1)	
La(2)−La(3)	4.244(1)	
La(2)−La(5)	3.754(1)	
La(2)−La(6)	3.922(1)	
La(3)−La(4)	4.221(1)	
La(3)−La(5)	3.884(1)	
La(3)−La(6)	3.612(1)	
La(4)−La(5)	3.799(1)	
La(4)−La(6)	3.945(1)	

[a] The notation follows the work of Schäfer and Schnering.[1] The letters e and f denote edge bridging and face capping atoms of atom type i, and a stands for coordination of corners of adjacent clusters. For example, Br(1) bridges the La(1)−La(2) edge in one cluster, and the La(4)−La(5) edge in an adjacent one. Thus, it is type e, and in both clusters, it acts as a bridging ligand, thus i-i. Br(2) caps the La(1)−La(2)−La(5) face and, thus, is type f. It is a terminal ligand to La(3) in an adjacent cluster, thus the notation i-a. Consider La(3) in the current cluster, it is also type a-i. Therefore a semicolon is used to separate these two types. See Figure 1.

Table 4. Extended Hückel Parameters

	orbital	H_{ii} (eV)	ζ_1[a]	ζ_2	c_1[a]	c_2
La	6s	−7.67	2.14			
	6p	−5.01	2.08			
	5d	−8.21	3.78	1.381	0.7765	0.4586
Br	4s	−22.07	2.588			
	4p	−13.1	2.131			
Fe	4s	−9.10	1.90			
	4p	−5.32	1.90			
	3d	−12.6	5.35	2.000	0.5505	0.6260

[a] Exponents and coefficients in a double ζ expansion of the d orbital.

procedure. The average Wigner−Seitz radius was 2.55 Bohr in the LDA computations. The EH parameters used in the computation are listed in Table 4.

Physical Property Measurements. For conductivity measurement, the polycrystalline samples were pressed into pellets of 5 mm in diameter and ca. 2 mm in thickness. The conventional four-contact method[36] was used. Susceptibility measurements were carried out on a Quantum Design PPMS 6000 magnetometer, using sample quantities of ca. 50 mg.

Results and Discussion

Crystal Structure. So far, all known reduced rare earth halides based on the octahedral RE_6Z unit are derived from the $RE_6X_{12}Z$ cluster with a cuboctahedral X atom arrangement above the edges of the octahedron. The packing of these clusters leads to vacancy variants of the rocksalt type structure. Some relevant structures are listed in Table 5. The structure of $La_6Br_{10}Fe$ is a first example of a significant variation from the known structures. It contains the familiar octahedral La_6Fe unit, however, only nine Br atoms lie above edges and three above faces of the octahedron. The La_6Fe octahedron is very distorted as shown in Figure 1. The La−La distances vary from 3.61 (La3−La6) to 4.24 Å (La2−La3). The La−Br distances of 2.97–3.67 Å are within the normal range as in many other reduced rare earth bromides. The main distortion is the contraction along the La5−La6 direction. Four corners of the octahedron (La1, La2, La3, and La6) are coordinated by two, one corner (La5) by one, and one (La4) by three Br atoms. The 9 bridged edges are La2−La5, La3−La5, La4−La5, La1−La6, La2−La6, La3−La6, La1−La2, La1−La4, and La2−La3. Out of the 12 Br atoms above the octahedron apexes, 4 also bridge the edge or cap the face of an adjacent La_6 octahedron and 8 are shared with another two La_6 octahedra, linking one corner and bridging one edge or capping one face of these two octahedral as shown in Figure 2.

Neglecting the Br atoms above the apex atoms, the discrete cluster has the composition $La_6Br^e{}_9Br^f{}_3Fe$ where e and f denote positions above the edges and faces of the octahedron, respectively. As the e-type atoms Br1 and Br10 are shared between adjacent clusters in the same functionality, the formula $La_6Br^e{}_5Br^e{}_{4/2}Br^f{}_3Fe = La_6Br_{10}Fe$ results. In the notation of Schäfer and Schnering[1] the complicated interconnection can be described as $La_6(Br^{a\text{-}i,i\text{-}a}{}_{6/2})^f(Br^{i\text{-}i}{}_{4/2}Br^{i\text{-}a,a\text{-}i}{}_{2/2}Br^{i\text{-}a,a\text{-}i,a\text{-}i}{}_{12/3})^eFe$ which also reduces to $La_6Br_{10}Fe$. The superscript i stands for the bridging and face capping Br ligands, while the notation a for the corner coordinating ligands. $Br^{a\text{-}i,i\text{-}a}$, therefore, is a ligand that is coordinated to the corner of the current La_6 octahedron but also bridges an

(36) van der Pauw, L. J. *Philips Res. Rep.* **1958**, *13*, 1.

Table 5. Lattice Constants (Length in angstroms and Angles in degrees) and Space Groups of Some Fe-Containing and 6–10 Type Reduced Rare Earth Metal Halides

compound	*a*	*b*	*c*	α	*β*	*γ*	space group	cluster type	ref
$La_6Br_{10}Fe$	8.255(1)		30.033(6)				$P4_1$	mixed M_6X_{12}/M_6X_8	this work
$Pr_7I_{12}Fe$	15.833(1)		10.734(1)				$R\bar{3}$	M_6X_{12}	17
$Gd_7I_{12}Fe$	15.492		10.624(2)				$R\bar{3}$	M_6X_{12}	17
$Y_7I_{12}Fe$	15.351(1)		10.661(1)				$R\bar{3}$	M_6X_{12}	17
$Pr_{12}I_{17}Fe_2$	11.798(4)	11.791(2)	9.830(2)	114.87(2)	104.82(4)	93.19(2)	$P\bar{1}$	M_6X_{12}	26
Gd_2Fe_2I	4.0143(5)		17.180(2)				$P6_3/mmc$	condensed trigonal prisms	24
$Pr_6Br_{10}Co$	9.359(4)	9.243(5)	7.538(3)	97.37(4)	107.3 l(4)	110.17(3)	$P\bar{1}$	M_6X_{12}	15
$Pr_6Br_{10}Ru$	9.206(4)	9.505(3)	7.606(4)	97.08(4)	107.47(4)	109.69(4)	$P\bar{1}$	M_6X_{12}	15
$Pr_6Br_{10}Os$	9.272(2)	9.486(3)	7.614(2)	97.09(2)	107.48(2)	109.83(2)	$P\bar{1}$	M_6X_{12}	15
$Y_6I_{10}Ru$	9.456(2)	9.643(2)	7.629(1)	97.20(2)	105.04(2)	107.79 (2)	$P\bar{1}$	M_6X_{12}	18
$La_6I_{10}(C_2)$	9.687(1)	9.728(1)	7.955(1)	97.34(1)	105.56(1)	107.81(1)	$P\bar{1}$	M_6X_{12}	27
$Ce_6I_{10}(C_2)$	9.588(1)	9.648(1)	7.875(1)	97.24(2)	105.32(2)	107.69(2)	$P\bar{1}$	M_6X_{12}	27

edge or caps a face of an adjacent octahedron. It bridges an edge or caps a face of the current octahedron but is coordinated to the corner of an adjacent octahedron. An example is Br(3) (see Figure 1), it bonds to the current La(6) corner and caps an adjacent La(1)−La(4)−La(5) face. It can also be considered as capping the current La(1)−La(4)−La(5) face and bonding to an adjacent La(6) corner. The $Br^{i\text{-}a,a\text{-}i,a\text{-}i}$ type ligands are shared by three La_6 octahedrons in the same sense. An example is Br(5) (see Figure 2), which appears three times in Figure 1. Table 3 classifies all the ligands in detail according to this system of notations.

The pronounced asymmetry of the Br coordination polyhedron around the La_6Fe octahedron has two important consequences. First, the La octahedron is heavily distorted, in first approximation squeezed along a 4-fold axis as described earlier. As seen in Table 3, the four La−Fe distances in the waist (La1−La2−La3−La4) of the octahedron are between 2.89 and 3.01 Å, whereas the La−Fe bonds to the "apical" atoms (La5−Fe and La6−Fe) are much shorter, 2.55 and 2.41 Å, respectively. This differentiation of the La−Fe distances is quite unusual and even exceeds that in $La_{12}I_{17}Fe_2$ where the distances 2.87 vs 2.71 Å have been found.[25] Second, the rocksalt-type arrangement, i.e., the common close-packing of Br atoms and the La_6Fe unit is lost. The rather dramatic difference of the common close-packing arrangements of I and Ru atoms in $Y_6I_{10}Ru$ on one hand and the irregular arrangement of Br and Fe atoms in $La_6Br_{10}Fe$ is obvious from Figure 3. The question arises what might be the driving force behind the distortion.

Electronic Structure. The distortion could be of electronic origin. A formal electron partition of $(La^{3+})_6(Br^-)_{10}Fe^{2-}\cdot 6e^-$ shows that there are 16 cluster electrons in the La_6Fe octahedron including those of (formal) Fe^{2-} and 6 electrons forming metal−metal bonds in the La_6 cage. Previous studies for the $RE_6X_{12}Fe$ cluster with the X atoms arranged above the RE_6 edges have shown that 10 of these electrons reside in the Fe 3d orbitals, and 6 in the a_{1g} and t_{1u} orbitals that are of La−La bonding character.[9,16,17,23] Therefore, the 16 electrons do not exceed the 18 electron limit imposed by these orbitals. As four electrons occupy the degenerate t_{1u} orbitals in the regular cluster, it could be susceptible to a Jahn–Teller distortion. A contraction along the local *z*-axis

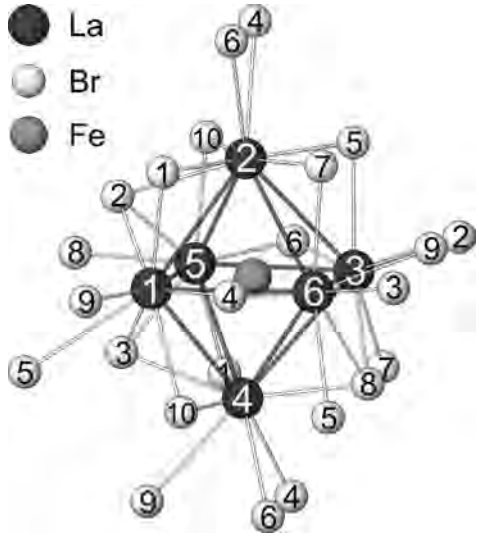

Figure 1. La_6Fe octahedron coordinated by Br atoms in the $La_6Br_{10}Fe$ structure. Atoms are numbered as in Tables 2 and 3.

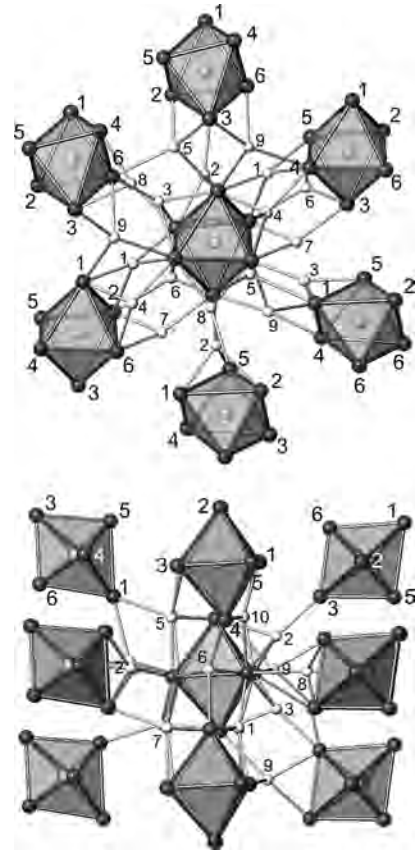

Figure 2. Arrangement of La_6Fe in the structure of $La_6Br_{10}Fe$ along the [0 1 0] (top) and along [1, 1, 0] (bottom) directions.

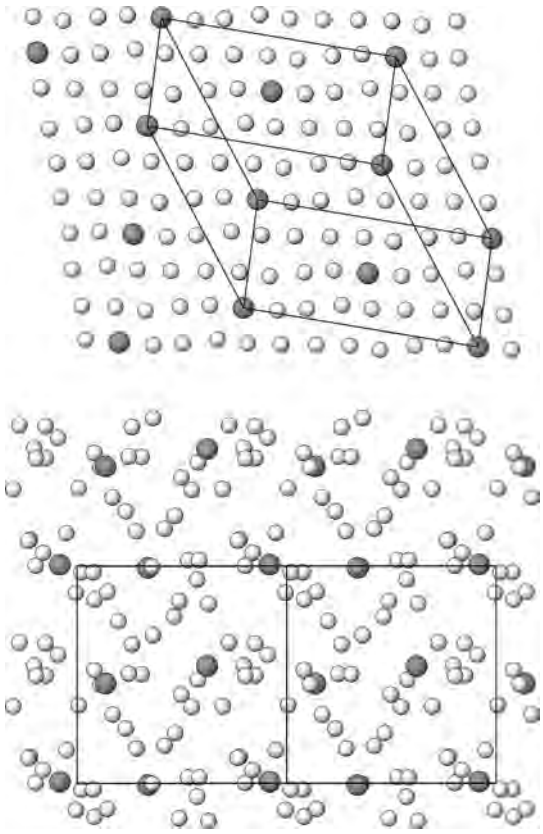

Figure 3. Comparison of the arrangements of I and Ru atoms in $Y_6I_{10}Ru$ (top)[18] with those of Br and Fe atoms in $La_6Br_{10}Fe$ (bottom). The structures are projected approximately along the [−1, −2, 3] and [1, 0, 1] directions, respectively. Dark spheres are Ru, Fe, and unit cells outlined.

will destabilize one of the three t_{1u} orbitals that have mainly Fe d_{xz}, d_{yz}, and p_z character and stabilize the remaining two. So far, the cluster core La_6Fe with halogen atoms above all edges of the octahedron has been considered. In order to take the unusual coordination by Br atoms above both edges and faces into account as it occurs in the $La_6Br^e{}_9Br^f{}_3Fe$ cluster, a systematic study at the EH level (without charge iteration) has been performed for different arrangements starting from empty La_6 cores. For simplicity and for the purpose of comparing with the classic Cotton−Haas orbital ordering,[37] we ignore the apical Br atoms. As is well-known, the effect of the addition of apical ligands is mainly the increase of the HOMO–LUMO gap, but the orbital ordering in the vicinity of the HOMO–LUMO energy range will remain the same.[9] Calculations with apical ligands (not shown here) indeed confirmed our expectation. The cage orbitals of bonding and nonbonding character are compared in Figure 4. The idealized La_6Br_{12} and La_6Br_{12} clusters have O_h symmetry, while the La_6Br_{9+3} and experimental clusters have C_1 symmetry.

The all familiar patterns of 8 and 12 obitals[37] for the regular La_6Br_{12} and La_6Br_8 clusters, respectively, are shown in Figure 4a and b. For the mixed $Br^{e,f}$ arrangement in the La_6Br_{9+3} cluster (Figure 4c and g), 13 orbitals are found in the energy range of the cage orbitals. Five of them are actually of Br p character, pushed to high energy because of (too) close contacts between Br^e and Br^f (2.58 Å). These states are therefore omitted in the figure. They are absent for the experimentally observed arrangement of atoms (Figure 4d and h) as they should be.

The occupation of the cluster centered by an Fe atom adds the e_g, t_{2g} blocks. In the case of the $La_6Br_{12}Fe$ cluster (Figure 4e), the number of cage orbitals with La−La bonding character is the same as in the empty cluster. However, the t_{2g}* set is of La−Fe antibonding and a_{2u} La−Br antibonding. The 18 electron limit is reached with the occupation of the t_{1u} orbitals.[16] It has been pointed out that the 18 electron limit is not strictly obeyed.[38,39] In the hypothetical La_6Br_8Fe cluster, too, the number of cage orbitals is preserved, and according to the above reasoning the t_{1u} orbital is the HOMO. Due to the deviation from O_h symmetry in the idealized $La_6Br_{9+3}Fe$ cluster (Figure 4g) and, even more in the distorted one, the degeneracy of the HOMO is removed.

Figure 5 is the calculated band structure of $La_6Br_{10}Fe$ using the LDA method where the Fermi level is set to be the zero point of energy. The relative energies of the bands deviate quite significantly from the EH−MO's, in particular concerning the a_{1g}; however, the general feature regarding the electron count is preserved. In the −2.3 to −1.9 eV region, there are four bands corresponding to the four a_{1g} orbitals of the four La_6Fe octahedra in the unit cell. In the −1.7 to −1.0 eV region, there are 20 Fe d bands. Because of the distortion, these split into four groups with the indicated energy order. Just below the Fermi level, there are 8 of the 12 t_{1u} derived bands, the other 4 are above the Fermi level as a result of the distortion. The LDA estimate of the band gap is approximately 0.7 eV corresponding to a semiconductor. This method, however, is well-known for underestimating the sizes of band gaps.

The Jahn–Teller effect would clearly favor a distortion of the cluster as observed in $La_6Br_{10}Fe$. However, it is questionable whether this effect is the only one or even the dominant effect. In $Th_6Br_{15}Fe$, the octahedron is regular in spite of a very similar bonding configuration except for one more cage electron compared to $La_6Br_{10}Fe$.[40] The cause for the distortion of the cluster in the latter compound has rather to be sought in the strongly varying coordinations of the La atoms by Br atoms. The earlier mentioned compounds $Pr_6Br_{10}Z$ (Z = Co, Ru, Os), $Y_6I_{10}Ru$ and $La_6I_{10}(C_2)$ exhibit (distorted) octahedral coordinations of all RE atoms by five halogen and the endohedral atoms. In contrast, the La atoms in $La_6Br_{10}Fe$ have coordinations by 5Br + Fe and 6Br + Fe, respectively. It seems that the radius ratio RE/halogen is a critical parameter, and subtle size effects are responsible for the enhanced coordination number of the large La atom.

Physical Properties. The physical properties of $La_6Br_{10}Fe$ are in agreement with the analysis of the chemical bonding described above. The resistivity measured in the temperature range from 5 to 300 K is in the order of 10 MΩ cm. Because

(37) Cotton, F. A.; Haas, T. E. *Inorg. Chem.* **1964**, *3*, 10.
(38) Payne, M. W.; Corbett, J. D. *Inorg. Chem.* **1990**, *29*, 2246.
(39) Mattausch, Hj.; Zheng, C.; Kienle, L.; Simon, A. *Z. Anorg. Allg. Chem.* **2004**, *630*, 2367.
(40) Böttcher, F.; Simon, A.; Kremer, R. K.; Buchkremer-Hermanns, H.; Cockcroft, J. K. *Z. Anorg. Allg. Chem.* **1991**, *598*, 25.

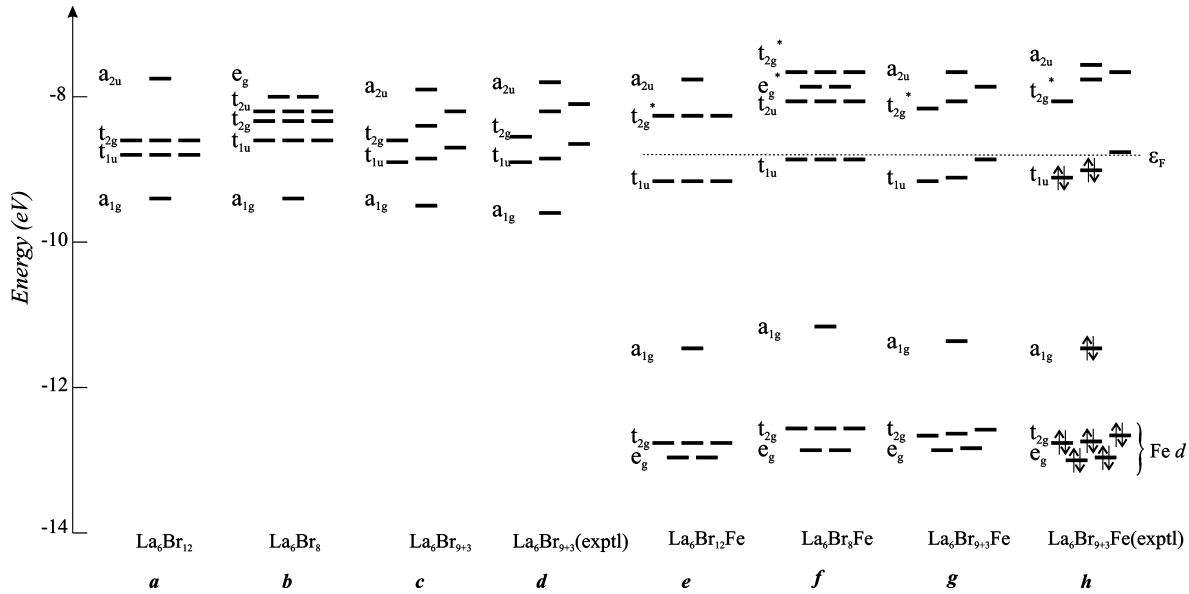

Figure 4. La−La bonding orbitals in the empty regular (a) La_6Br_{12}, (b) La_6Br_8, (c) La_6Br_{9+3}, and (d) the experimental La_6Br_{9+3} clusters, as well as the corresponding Fe-centered species (e−h). The symmetry labels for the idealized La_6Br_{9+3} and experimental La_6Br_{9+3} clusters denote the corresponding orbitals in the octahedron clusters from which they are derived.

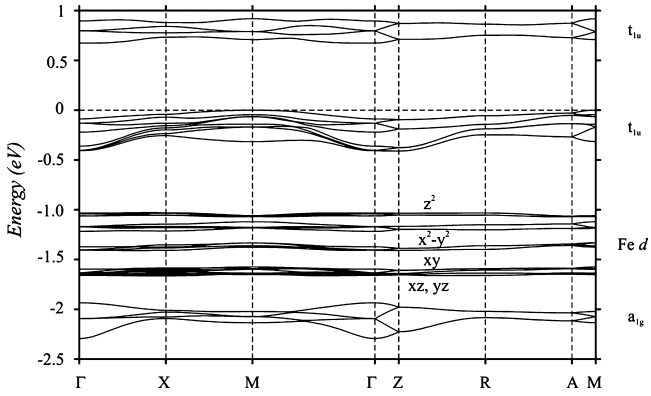

Figure 5. Band structure of $La_6Br_{10}Fe$ calculated by the LDA method.

of the high value, the measurement had large fluctuations. Both the results of band structure calculations and measurement are in agreement with expectation as the discreteness of the cluster due to interconnection via nonmetal atom bridges in all surrounding corners generally results in insulators or semiconductors.[6] The magnetic susceptibility measurement revealed nonmagnetic behavior ($\chi \approx 0$) after correction for an impurity which orders ferromagnetically at 155 K saturating in a field of 7 T. The magnetic behavior of $La_6Br_{10}Fe$ is consistent with the closed-shell electron configuration as discussed.

Conclusion

A new reduced rare earth metal halide $La_6Br_{10}Fe$ has been synthesized. Its structure represents a novel mixed M_6X_{12}/M_6X_8 type that has not been observed previously. The cluster is characterized by a significantly distorted RE_6 octahedron. Because of the discreteness of the clusters in the structure, the compound is an insulator.

Acknowledgment. We thank R. Bailey for assisting the EDX measurement, E. Brücher for the magnetic susceptibility measurements, G. Siegle for the conductivity measurements, and C. Kamella for help with the drawings.

Supporting Information Available: Listing of X-ray crystallographic details in CIF format. This material is available free of charge via the Internet at http://pubs.acs.org.

IC701229Q